Westinghouse Advanced Reactors Division

P8230

DISCLAIMER

WARD-4210T1-1

WARD-4210T1-1

UC-25

SODIUM TECHNOLOGY PROGRAM

PROGRESS REPORT FOR THE

PERIOD ENDING NOVEMBER 30, 1970

Carbon Equilibrium Loop Continuation

Approved by: William E. Ray

W. E. Ray
Principal Investigator

P. Murray

P. Murray
Project Manager

Prepared for the U.S. Atomic Energy Commission
Division of Reactor Development and Technology
Under Contract No. AT(30-1)-4210, Task 1, Subtask B.

Submitted to AEC/NYOO in January 1971

Westinghouse Electric Corporation
Advanced Reactors Division
P. O. Box 158
Madison, Pennsylvania 15663

Printed in the United States of America
Available from
National Technical Information Service
Springfield, Virginia 22151
Price: Printed Copy $3.00; Microfiche $0.65

TABLE OF CONTENTS

TABLE OF CONTENTS (CONTINUED)

LIST OF FIGURES

LIST OF TABLES

SECTION 1

INTERSTITIAL TRANSPORT IN SODIUM SYSTEMS

C. Bagnall, B. R. Grundy, S. Orbon, S. L. Schrock, and S. A. Shiels

1.0 OBJECTIVES

The objectives of this program are to provide experimental information and analytical relationships for design data so that the rate and direction of carbon and nitrogen transfer and the associated mechanical property changes of structural materials within liquid metal systems, representative of primary and secondary sodium systems, may be predicted.

2.0 PRIOR WORK

2.1 Related Work Outside Westinghouse

The current AEC sponsored interstitial transfer program is part of an overall national program on sodium technology. The work at Westinghouse interfaces with, and in some areas complements, work being performed at WADCO, AI, ANL, BNL, and GE. Programs at MSAR and UNC, which have now been terminated, are also relevant to the Westinghouse effort.

In the important area of carbon meter calibration and operation, the Westinghouse program will benefit from past work at UNC and BNL where the meters were developed, and at MSAR where the UNC meter was used successfully in high carbon environments. The ANL program is perhaps the most extensive one outside Westinghouse. ANL personnel are concentrating primarily on relating carbon transport to chemical species and on adapting experimental meters for on-line use in EBR-II. The meter program is of particular interest to Westinghouse.

The work at AI, where an investigation will be conducted on the effects of the carbon and nitrogen content in stainless steel on the mechanical properties of the steel, will interface with the work at Westinghouse in the area of material properties. Work related to this contract, being performed by WADCO, is in the equipment design and installation phase.

2.2 Preparatory Work

During the first half of FY-1970, extensive preparatory work on the interstitial transport program was performed in anticipation of the current AEC contract. This work involved a preliminary survey of the literature and identification of the key problems in defining interstitial transfer in sodium systems. An experimental approach was decided upon, and a facilities design concept was originated. The program and design philosophies were embodied in the work program which was submitted in November 1969.

A state of the art review of carbon and nitrogen diffusion data first issued as an internal memo in September 1969 has been expanded and is included as Appendix B of this report.

2.3 Facilities

The design of the experimental facilities, designated as Carbon Equilibrium Loops (CEL's), including the control panels and tie-in of all on-line instrumentation was completed, and a System Design Description (SDD) was written. The SDD, together with the relevant detailed drawings, was submitted to the AEC, Coolant Chemistry Branch, for approval. Apart from minor modifications, the SDD was accepted.

2.4 On-Line Metering

All outstanding bids and information for on-line sodium impurity metering equipment were received, enabling final choices to be made. Devices incorporated are as follows:

1. UNC diffusion carbon meter
2. BNL electrochemical carbon meter
3. Westinghouse electrochemical oxygen meter
4. Fisher Gas Partitioner (chromatograph) for cover gas hydrogen monitoring

3.0 CURRENT PROGRESS

3.1 CEL-1

Construction of CEL-1 was completed, the system was filled with sodium, and flow was achieved in all by-pass lines. Difficulties with maintaining flow were experienced; however, during subsequent operation, various other design faults were revealed. The problems and the steps taken to correct them are described below.

1. The by-pass loop for the BNL meter was redesigned to eliminate potential gas pockets and to facilitate complete draining. The trace heaters on the probe housing were changed to allow independent heating of this region. This simplified probe removal. At the same time, the UNC meter side-arm orientation was changed to allow easier access to other loop components.
2. A valve on the BNL meter side-arm seized and had to be replaced.

3. One of the requirements of the ARD Stored Energy Committee was that the loop should dump under positive pressure rather than the original specification which called for a simple dump under gravity. The positive pressure system requires that the dump tank vents be slightly above atmospheric pressure on the dump signal. Problems were experienced with sodium vapor or aerosol plugging the small diameter gas lines and the solenoid valves on the dump system. This plugging was eliminated by replacing the 1/4 inch lines with 1/2 inch stainless steel tubing and installing a simple fiberglass filter before the valves. A similar filter was used successfully on the cover gas outlet line leading to the gas chromatograph.

4. The location of the oxygen meter, in parallel with the cold trap, made it difficult to control the oxygen meter temperature. The meter was therefore moved from this location and installed in a separate by-pass line with the addition of an economizer and an air blast cooler.

   It is now possible to run the oxygen meter at 700°F while the main loop temperature is in excess of 1200°F.

5. A valve downstream of the cold trap was found to maintain a temperature lower than the trap. Consequently, plugs tended to form at the valve, especially when the sodium contained a high level of hydrogen. The problem was eliminated by installing a clam shell heater on the cold trap outlet line and ensuring that the sodium entering the valve was at a higher temperature than the cold trap.

The alterations described above appear to have solved the CEL-1 operational difficulties.

3.2 CEL-2

Work on construction of CEL-2 was suspended for two months due to uncertainties regarding future direction of the contract. Work on this loop was resumed with the identification of funds covering the remainder of CY-1970.

The piping layout of CEL-2 was changed to make access to loop components easier, and the design changes required on CEL-1 were incorporated into the new loop layout. All component parts have been machined and welding of the components is about 95% complete.

3.3 Loop Operation

CEL-1 was filled and brought into operation at the beginning of September. During the period September-October most of the alterations described in the previous section were made involving approximately three weeks of down time. The remainder of the time was used to obtain operational experience on the loop and the meters. Meter performance is reported in a separate section. Procedures were developed for changing both the carbon meter and

the oxygen meter probes as well as for loading and unloading specimens. Also, in collaboration with the Analytical Chemistry Group, procedures for determining oxygen levels using the on-line vacuum distillation unit were developed.

The principal operational problem at this time is controlling the hydrogen which accumulates in the system during operation of the UNC carbon meter. The cold trap system is relied on as the major means of controlling the hydrogen level; and under steady state operation at 1200°F, the cold trap will hold the hydrogen at a level equivalent to $\sim$ 30 ppm in the cover gas (Purging at 1 cu. ft/hr at 30 psi) as measured by a gas chromatagraph. However, the cold trap will not handle sudden surges of hydrogen. During one operation the cold trap plugged at the control valve and flow was interrupted in the cold trap by-pass line. The UNC carbon meter was in operation during this time, but the cover gas hydrogen level did not rise above $\sim$ 36 ppm. When flow was re-started in the cold trap line, the hydrogen level peaked at about 350 ppm. Presumably, hydrogen had accumulated in the cold "dead leg" of the cold trap. The cold trap system could not handle this hydrogen level and plugged at temperatures as high as 500°F.

A similar situation occurred when attempts were made to start up the hot trap system. Prior to starting up the hot trap by-pass system, the cold trap was shut off to contain the trapped oxygen. Once again the "dead region," in this case the hot trap line, had accumulated large amounts of hydrogen. When the cold trap was restarted, it could not handle the hydrogen without plugging. In each case the hydrogen was cleared from the system by shutting off the UNC meter and flushing out the cold trap. The hydrogen eventually diffused out through the 1200°F containment walls. When the hydrogen reached a managable level the cold trap temperature was reduced.

During future operations, cold trapping will be continuous while the UNC meter is in operation, and any side loops which are not in use continuously will be periodically purged of hydrogen. Also, the UNC meter will be used on an intermittent basis only.

3.4 On-Line Metering

Since the last report (June 1970) all the proposed metering devices were obtained and installed on CEL-1. The following are details of the performances to date of each meter.

3.4.1 UNC Diffusion Carbon Meters

Delivery was made of two side loops and housings with probes as manufactured by UNC. The first of these was installed in CEL-1 taking the precaution described by UNC.[1] In addition to the fuel, air, and decarburizing gases formulated to conform to UNC recommendations, two gas mixtures for checking performance of the flame ionization detector (FID) and catalytic convertor were procured. Those mixtures contained approximately 200 ppm of both CH_4 and CO and 4000 ppm of CH_4 and CO.

No difficulty was experienced in removing the dummy probe and inserting the carbon meter probe in its place.

The two control consoles (temperature control and gas supply and analysis) were previously used by MSAR, and several of the idiosyncrasies described by Rodgers and Shrive[2] have appeared in the present work which includes the following:

1. At the fuel and air pressures suggested by UNC (9 and 15 psi, respectively) for the FID, the flame goes out with every re-routing of gas flow. The pressures used by Rodgers and Shrive[2] were adopted (14 and 15 psi) which gave improved sensitivity, but the flame still goes out with certain gas re-routing operations.

2. The humidifier temperature was set to give a water content in the decarburizing gas corresponding to a dewpoint of 27°F. This dewpoint varied with ambient temperature. Following the procedure of Rodgers and Shrive[2] the dewpoint was raised to a nominal 47°F. Readings since have been in the range 47-48°F.

3. Small step changes in the FID output occur under steady state operational conditions. The frequency of these changes has diminished since raising the water content of the decarburizing gas.

4. The combinations of needle valve and rotameter used for gas flow control were unsatisfactory. Sticking floats, floats unresponsive to changes in flow, and inability to set a required flow were some of the symptoms. It proved impossible to calibrate the FID or check the catalytic convertor. This serious deficiency was overcome by installing a Matheson Linear Mass Flowmeter with electrical readout immediately before the FID. Accurate flow measurement is now possible and has shown that a particular flow cannot be easily set with the needle valves. Since a change in FID output with gas flow has been noted, it was necessary to calibrate FID output versus flow rate for small flow deviation either side of the required value of 12.5 cc/min.

A calibration of the FID was obtained using the methane fraction of the calibration gases. 100% efficiency was confirmed for conversion of the CO fraction of the calibration gases to CH_4 by the catalytic convertor. These results are plotted in Figure 1-1. The curve is identical with that indicated as typical by UNC.[1]

3.4.2 BNL Electrochemical Carbon Meter

Three meters were supplied by BNL incorporating a carbonate electrolyte and a graphite reference electrode. A housing was not included, therefore it was necessary to design one. It was fabricated from one-inch diameter stainless steel tubing. Sodium flows into the bottom and out of a side arm positioned eight inches above the end of the meter probe. This complies

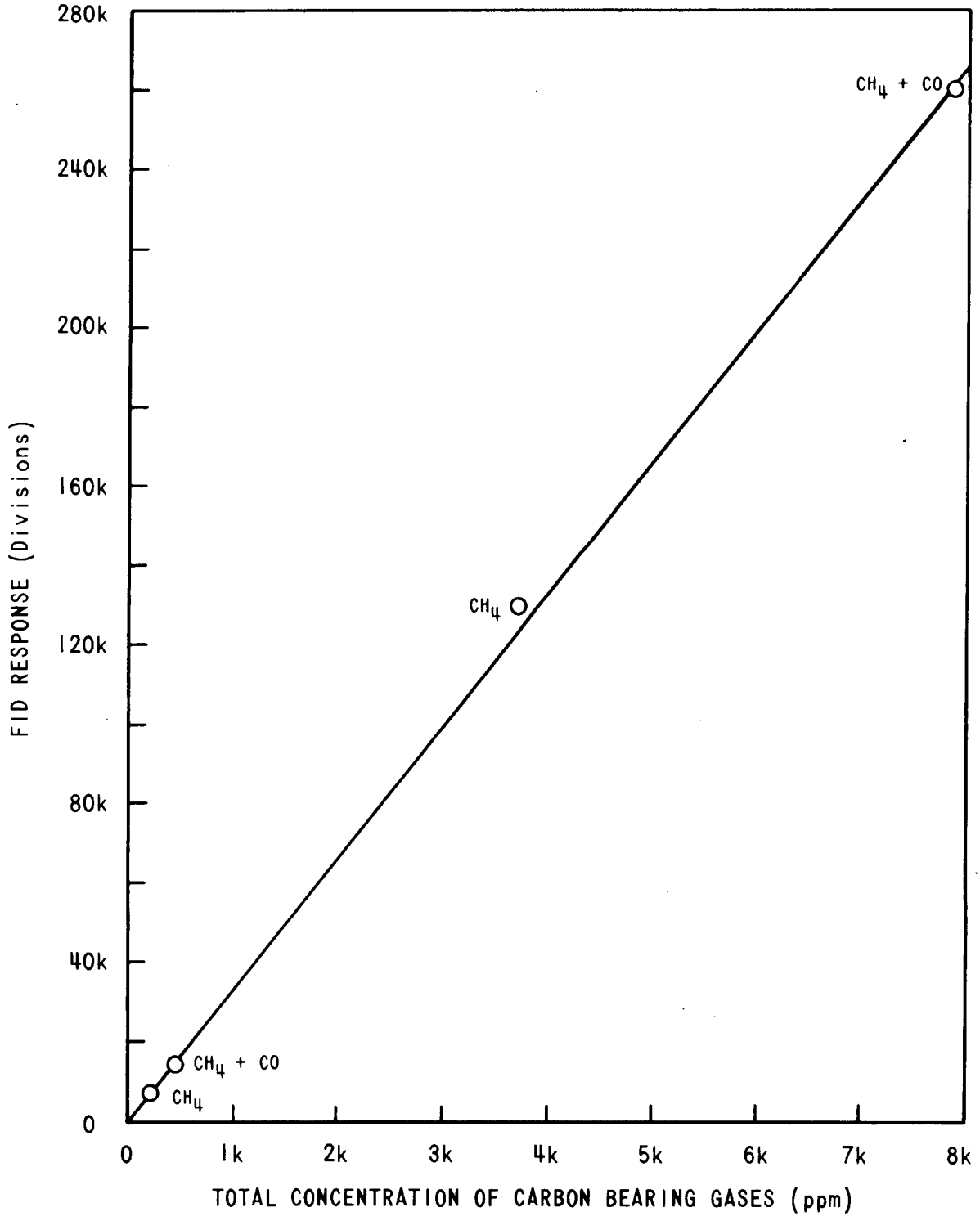

Figure 1-1. Flame Ionization Detector Calibration

3992-1

with the BNL recommended minimum immersion depth of six inches. The meter probe is sealed in place by a one-inch diameter Conoseal, and a gas space normally separates the seal from the sodium. A gas line to this space is provided and connected into the cover gas system. This permits gas venting and pressure equalization across the probe diaphragm when necessary. A heater/cooler system was included in the sodium inlet line to the housing. This was designed to maintain the meter in its recommended operational temperature range of 1145-1200°F with the main loop between 800 and 1400°F.

When the first meter was brought to temperature, it was found to have an internally open circuit. It is probable that this damage occurred during transport although the meters were carefully packed. Installation of the second meter proved difficult, and it was decided to alter the geometry of the BNL side arm. Establishing flow after these changes was also difficult, and the meter was subjected to a considerable pressure differential when the gas line became blocked with sodium. This meter was also open circuit at temperature. The damage almost certainly resulted from the operational difficulties described above. Upon removal, the bottom of the iron membrane (10-mil thick with reinforcing ribs) was seen to be dished. Installation of the third meter and establishment of flow was straightforward. An EMF in the expected range (typically, 0.030V at 1200°F) quickly appeared.

BNL has indicated that mass transfer of iron through the molten electrolyte has been observed, resulting in growth of a whisker which can short the reference electrode to the iron diaphragm. This short developed unexpectedly early in the meter's life and subsequently, on three more occasions. The shorts occurred after 280, 333, 458, and 516 hours of operation. A total of 530 hours operation has been reached (December 1, 1970). The short is easily corrected by loosening the center electrode coupling at the upper part of the meter and rotating the electrode with the electrolyte molten. After breaking the whiskers, several hours are required for full recovery of EMF.

Presence of hydrogen in the loop deriving by diffusion from the decarburizing gas mixture used with the UNC carbon meter has also been observed to affect the electrochemical carbon meter. It should be noted, however, that the initial short by iron whiskers occurred before starting of the UNC meter. When hydrogen is observed in the cover gas, a depression of the EMF occurs. On one occasion large amounts of accumulated hydrogen from the cold trap, when passed into the loop, gave rise to as much as 350 ppm hydrogen in the cover gas. A corresponding depression of BNL meter EMF to 0.004 V was observed. When the hydrogen was removed, the meter recovered. It should be noted that the effect appears directly on the meter and not an interaction of hydrogen and carbon in sodium solution. Such an interaction would be expected to reduce carbon activity and, therefore, give an increased EMF.

Operation of the BNL carbon meter and the UNC carbon meter simultaneously on a small loop appears very difficult because of the hydrogen inserted into the loop by the UNC meter.

3.4.3 Westinghouse Electrochemical Oxygen Meter

The Westinghouse oxygen meter was installed so that part of the cold trap side loop was common to both devices. A bypass arrangement enabled either cold trap or meter flow to be obtained independently and a pre-cooler was used to keep the meter temperature below 1000°F.

Operation of the meter of necessity has been limited by the stage reached in a ceramic electrolyte development program at WADCO, in cooperation with the commercial supplier, Zirconium Corp. of America. Three meter probes incorporating electrolyte (ThO_2 - 7-1/2% Y_2O_3) representative of an intermediate stage in development were operated. The improvement lay in reducing impurity content. This was achieved on a bulk basis, but at grain boundaries higher impurity concentration than before has been observed. Meter performance was unsatisfactory; all developed large temperature coefficients quickly (up to - 1.0 μ V/°F) rendering the meter "noisy" and this was associated with poor sensitivity.

It became apparent that temperature control was inadequate, and modifications described in an earlier section have been made to alleviate the situation in anticipation of improved meter probes. The meter now operates in its own side loop and has a tube and shell heat exchanger giving good temperature stability.

Isostatically pressed, high purity, ceramic electrolytes are now becoming available, and preliminary tests elsewhere indicate excellent meter characteristics. A meter incorporating this type of electrolyte is to be installed in the near future.

3.4.4 Cover Gas Hydrogen Monitoring By Gas Chromatograph

The Fisher Gas Partitioner Model 29 has been installed to monitor cover gas hydrogen content. Hydrogen is introduced into the sodium by diffusion from the decarburizing gas of the diffusion carbon meter.

In preliminary laboratory tests, it was established that the limit of detection was 5 ppm hydrogen using argon carrier gas and a 5 ml. sample. The chromatograph was modified to provide automatic, time sample injection using a Varian solenoid operated sampling valve and a solid state timer. On the loop, the whole cover gas sweep of 1 cu ft/hr is passed through the sampling valve continuously, and samples are injected every 3 minutes. The cover gas is taken from the sample tank via a two stage sodium vapor/aerosol filter. An earlier single stage filter required modification since it blocked in 24 hours with the loop operating at 1200°F. Two standard calibration gases are available and can be fed to the meter as required.

Operation of the system has been satisfactory. The chromatograph responded rapidly to those changes in loop operation which caused hydrogen peaks such as initiation of flow in previously static by-pass loops within one four minute sampling cycle. Unequivocal indication of hydrogen has been very useful in showing potential dangers including: tendency of hydrogen to accumulate in static side loops unless maintained at high saturation temper-

atures; and detrimental influence of hydrogen on the electrochemical carbon meter. It has also shown that diffusion through containment at 1200°F can be used to remove hydrogen from the system, as an earlier analysis indicated.[3] Under dynamic steady state conditions, with no cold trapping, the indicated hydrogen level has fallen in the range predicted by the analysis,[3] assuming efficiency of hydrogen stripping by the cover gas lies between 10 and 100%.

3.5 Sodium Analysis

3.5.1 Determination of Oxygen by On-Line Vacuum Distillation

During this report period two successful on-line distillation analyses were performed while the CEL-1 was operating at 720°F with the by-pass sample and distillation lines at 630°F during sampling. The analyses were performed immediately prior to and after the first experimental run. Each time the distillation chamber and sample crucible were throughly degassed prior to allowing sodium to flow over the crucible for 20 minutes. The crucible was then withdrawn into the induction coil field, the sampling well valved off, and the sample was distilled at 700°F for one hour. By-pass samples were taken after the removal of the crucible from the sampling well five minutes after the first distillation sample was taken and thirty minutes after the second sample. Table 1-1 shows the results obtained on the samples for each analysis. Further analyses will be performed by on-line distillation to establish the procedure.

Table 1-1. CEL-1 SODIUM ANALYSIS BEFORE AND AFTER RUN NO. 1

		Before Run (ppm)	After Run (ppm)
Vacuum Distillation	O_2	2-4	10
By-Pass Sampling	O_2	7.5 $\pm$ 1.3	8.2 $\pm$ 1.4
	N_2	1	1
	C	9	14

3.5.2 Determination of Nitrogen and Carbon

The ARD procedures for the measurement of carbon and nitrogen in sodium metal were accepted as interim methods until the committee to review sampling and analytical methods reaches agreement on the ANL interim methods manual.

Carbon and nitrogen analyses were performed on the by-pass samples before and after the first experimental run. The values obtained are given in Table 1-1.

3.6 Experimental Work

Type 304 stainless steel foil specimens were mounted on the nine bobbins, two to a bobbin, and loaded into the sample tank on October 22. Prior to mounting, the 2-3/4" x 1", three mil foil strips were lightly abraided, degreased, washed, dried, and weighed. The exact location of each specimen in the sample tank was recorded. The loop ran at steady state conditions at about 720°F, cold trapping at 300°F, for 20 hours after which a sodium by-pass sample and the first vacuum distillation sample were taken. The first run was then initiated by increasing the operating temperature to 1200°F. These conditions were maintained for 265 hours. Based on available diffusion data, the 265 hours at 1200°F was considered sufficient to achieve near equilibrium conditions in the 3 mil foil. The UNC meter read 31.5 FID units and cold trapping at 300°F was conducted continuously during this period.

After completion of the test, the samples were removed from the loop and weight change data were obtained from the specimens in an attempt to relate net interstitial change, as determined by analyses, to a loss or gain in mass. It was assumed that alteration of metallic alloy composition over a short time period is negligible. For example, a net combined loss of 500 ppm carbon and nitrogen from a one gram sample should be measurable as a weight loss of about 0.0005 grams.

Although all of the specimens, with one exception, showed a weight loss of about 5×10^{-4} grams per gram of material, it does not represent an interstitial change since a net gain was recorded by chemical analysis. A combination of mass transfer, oxide removal, and possibly humidity changes in the laboratory atmosphere between the time of the two weighings may have caused the weight changes.

Post exposure interstitial analyses (Table 1-2) showed some variations with regard to specimen pairs and specimen location. However, these were of a random nature, and no gradient or local concentration effects in the sample tank could be identified.

With two exceptions, the measured carbon levels in the foils after exposure fell within the range 532 ± 65 ppm. This represents an increase over the initial level (340 ± 30 ppm) of 100 ppm minimum up to a maximum possible increase of 290 ppm.

Nitrogen data established on the foil material covering over 70 separate determinations gave an as-received concentration of 929 ± 64 ppm. After sodium exposure in the above experiment, analyses from the 18 foil samples gave statistical data of 928 ± 63 ppm. The absence of significant change may be explained if it is assumed that the inner wall surfaces of the containment tubing have a nitrogen concentration at a similar high level to that finally present in the Type 304 stainless steel foil. The second run in CEL-1 is now under way. This experiment is basically a repeat of the first with the loop set at 1200°F for two weeks. However, an effort was made to lower carbon and nitrogen concentrations in the system by hot-trapping at 1100°F for one week prior to loading the specimens.

Table 1-2. Type 304 Stainless Steel Sample Data

After Exposure in CEL-1 245 hr/1200°F

Sample No.	Tube No. and Locations	Weight Loss (%)	Interstitial Content after 245hr/1200°F	
			Carbon (ppm)	Nitrogen (ppm)
S4/A	11-T	--	554	939
S4/B		--	450	1063
S4/C	13-B	0.055	503	967
S4/D		0.047	479	916
S4/E	12-C	0.066	516	1009
S4/F		0.064	513	946
S4/G	13-C	0.047	533	915
S4/H		0.047	468	769
S4/I	12-B	0.064	572	952
S4/J		0.045	499	849
S4/K	11-B	0.045	490	924
S4/L		0.055	561	937
S4/M	12-T	0.046	602	911
S4/N		0.046	578	839
S4/O	13-T	0.045	568	941
S4/P		0.046	744	833
S4/Q	11-C	NIL	510	945
S4/R		0.027	545	943

Notes:

As-received interstitial contents determined as:

Carbon 340 ppm $\pm$ 30

Nitrogen 929 ppm $\pm$ 64.

Tube numbers identify the three sample tubes; specimen location in sample tank is noted by T(top), C(center) and B(bottom).

Type 304 stainless steel foil specimens, together with three foils of Armco Iron, have been placed in the sample tank. UNC carbon meter readings will be made periodically with the side-arm temperature at various settings between 1000° and 1400°F. During its operation, continuous cold trapping will be used to ensure that hydrogen buildup in the loop is kept to an absolute minimum.

Figure 1-2 shows the change in microstructure occurring after exposure of the Type 304 stainless steel foil in sodium for 265 hours at 1200°F. The micrographs were taken from the central region of taper sections through the three mil foil. The major alteration as a result of the exposure appears to be formation of an equiaxed grain structure and second-phase precipitation at grain boundaries.

Experiments planned for the next quarter are expected to produce several calibration points for the carbon meters and show the relationship between carbon meter reading, temperature, and material type for some of the specimen materials.

3.7 Thermodynamic Modeling

Some effort has been directed towards establishing a theoretical model for interstitial transfer in sodium systems. The approach taken is to develop computational techniques using classical thermodynamics for the determination of equilibrium carbon profiles in a closed stainless steel loop system under an arbitrary temperature profile and to later modify this by introducing kinetic effects. The combination of the thermodynamic and kinetic treatments will lead to a computational method of predicting carbon and eventually nitrogen levels and profiles in a kinetic nonequilibrium situation.

3.7.1 Derivation of Model

Work during this reporting period has been concerned with the thermodynamic model only. A mathematical model of a closed, all austenitic loop was constructed and analyzed from the point of view of classical equilibrium. Based on this analysis, a computer program was written to calculate an equilibrium carbon concentration profile in a hypothetical loop. The complete analysis is given in Appendix A and is summarized below.

Definitions and assumptions made in this analysis are as follows:

1. The chemical potential for an isothermal volume element is constant across the sodium-stainless steel interface.[4]

2. A mass balance contraint is obeyed, i.e., the initial and final total carbon contents of the system must be the same.

3. The major metallic element concentrations do not change.

4. The standard state for carbon in both the sodium and the steel is regarded as graphite.

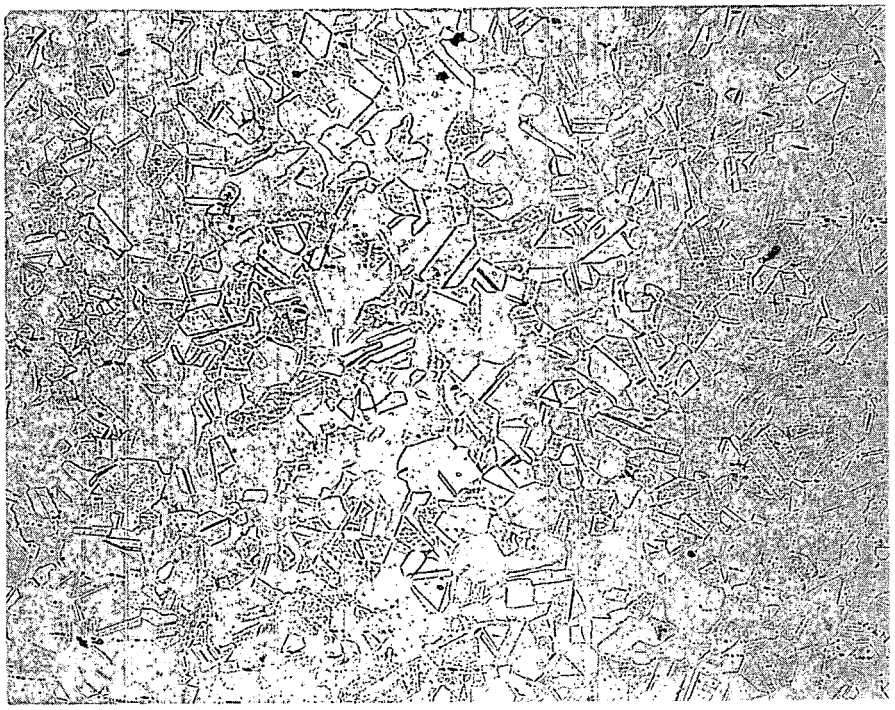

AS-RECEIVED

OXALIC ACID ETCH

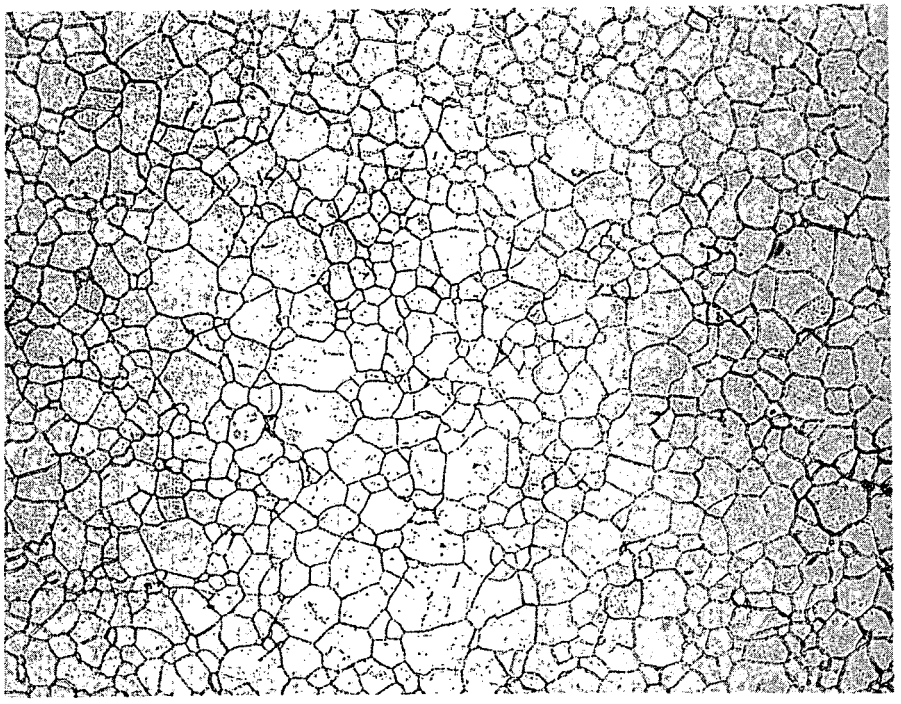

AFTER EXPOSURE

HF/HNO_3/GLYCEROL ETCH

Figure 1-2. Effect of 265 Hours Sodium Exposure at 1200°F on Type 304 Stainless Steel Foil. (Micrographs were taken from central regions of taper sections through the foils) (250x)

3992-2

5. The carbon content of the sodium is assumed essentially constant throughout the system.

Two conditions must be satisfied for any developed model. First, for any volume element of sodium δV^{Na} in 'equilibrium' with a volume element of stainless steel δV^{St} at a temperature T

$$\mu_i^{Na} = \mu_i^{\gamma}$$

where μ_i^{Na} and μ_i^{γ} are the chemical potentials of species in the sodium and the steel, respectively.

The second condition is the mass balance constraint where:

$$M_i^{\gamma} + M_i^{Na} = M_i \text{ total}$$

where M_i is the mass of species i.

Using thermodynamic data reported in the literature for the activity of carbon in steel[5] and in sodium,[6] three principal equations were developed which allow the calculation of the amount of carbon in the steel and in the sodium at any temperature T.

$$X_c^{Na} = \frac{1}{RT_{max}} \exp\left\{RT_{max}\ln X_c^o + (15206+3T_{max}+1300X_{Cr}^2) - (3450+7.5T_{max})(1-X_c^o)^2 - 27000X_{Cr}(1-X_c^o)\right\}$$

where X_c^{Na} is the carbon content of the sodium.

$$X_c^{\gamma}(T) = X_c^o \frac{k(T)}{k(T_{max})} \exp\left\{\frac{\alpha(X_{Cr})}{RT_{max}}\right\} \exp\left\{\frac{\alpha(X_{Cr})}{RT}\right\}$$

where X_c^{γ} is the carbon content of the steel at any temperature.

$$X_c^o = \bar{X}V \Big/ \int_o^L \frac{k(T)}{k(T_{max})} \exp\left\{\frac{-\alpha(X_{Cr})}{RT_{max}}\right\} \exp\frac{\alpha(X_{Cr})}{RT(x)} A(x)dx$$

where X_c^o is the carbon content of the steel at the highest temperature.

A computer program was written to perform the calculations and plot the results. The numerical intergration was performed by use of a trapezoidal technique using Rombergs extrapolation method[7].

3.7.2 Application of the Model

An arbitrary temperature profile, with temperatures between 700-1400°F, was assumed for a simple monometallic (Type 304 stainless steel) single tube system, and the above analysis was applied to it. The temperature profile is shown in Figure 1-3 together with the resulting carbon profile.

The analysis predicts that, for a system with an initial carbon level of 500 ppm;

1. All areas above about 800°F will lose carbon and below this temperature, will pick up carbon.
2. At the highest temperature, 1400°F, the equilibrium value will be approximately 5 ppm.
3. The predicted carbon level of the sodium is about 10^{-4} ppm, which is below the solubility limit and substantially less than measured sodium carbon contents.

Several factors which may lead to error have not been included in this preliminary treatment. The major assumption was, of necessity, that the system is a purely thermodynamic one, and kinetics have not been considered. In colder regions, the sodium may not be in equilibrium with stainless steel but rather with deposits of very different chemistry.

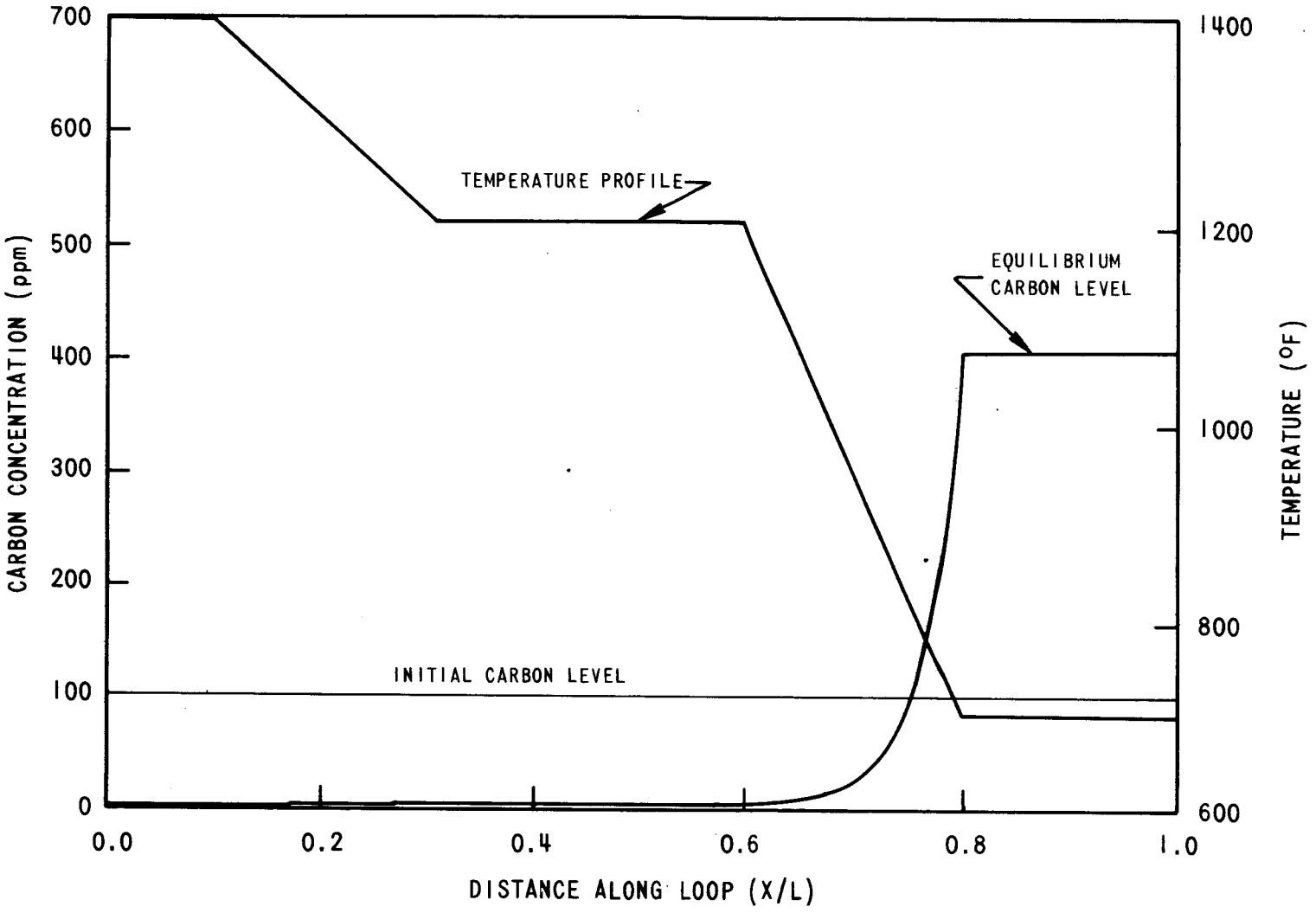

Figure 1-3. Carbon Profile Resulting From the Shown Temperature Profile

4.0 REFERENCES

1. W. Caplinger, "Carbon Meter for Sodium. Final Report," UNC-5226, March 1969.

2. S. J. Rodgers and R. J. Shreve, "The Effect of High-Temperature Sodium on the Mechanical Properties of Candidate Alloys for the LMFBR Program. Techniques for Monitoring High Carbon Activity Sodium: An Evaluation of the UNC Carbon Meter. Topical Report No. 16," MSAR-70-54, May 1970.

3. "Sodium Technology Program. Quarterly Progress Report for the Period Ending March 31, 1970," WARD-4173-1, May 1970.

4. K. G. Denbigh, The Principles of Chemical Equilibrium, Cambridge University Press, New York, 1961.

5. C. Stawstrom and M. Hillert, "Improved Depleted-Zone Theory of Intergranular Corrosion of 18-8 Stainless Steel," J. Iron Steel Inst. London 207, Pt. 1, pp. 77-85 (1969).

6. K. Natesan and T. F. Kassner, "Calculations of the Thermodynamic Driving Force for Carbon Transport in Sodium-Steel Systems," ANL-7646, December 1969.

7. IBM Application Program-System/360 Scientific Subroutine Package (360A-CM-03X) Version III, Programmers Manual, 4th Edition, International Business Machines Corporation, New York, 1968.

APPENDIX A
THERMODYNAMIC MODELING CALCULATIONS

S. Orbon

1.0 ASSUMPTIONS

The following restraints and assumptions were made in the development of the carbon transfer model.

1. The chemical potential for an isothermal volume element is constant across the sodium-stainless steel interface.[1]
2. A mass balance constraint is obeyed; i.e., the initial and final carbon contents of the system must be the same.
3. The major metallic element concentrations do not change.
4. The standard state for carbon in both the sodium and the steel is regarded as graphite.
5. The carbon content of the sodium is assumed to be constant, independent of temperature.

2.0 THE MODEL

Consider a volume element of sodium δV^{Na} in equilibrium with a volume element of stainless steel δV^{γ} at a temperature T.

At equilibrium,

$$\mu_i^{Na} = \mu_i^{\gamma} \tag{1}$$

Expanding,

$$\mu_i^{o\ Na} + RT \ln a_i^{Na} = \mu_i^{o,\gamma} + RT \ln a_i^{\gamma} \tag{2}$$

where: μ_i^{o} = the standard state of the i th species

superscript Na denotes sodium

superscript γ denotes austenitic stainless steel

a_i = activity of the i th species

Solving Equation 2 for a_i^{γ} gives

$$\frac{a_i^{\gamma}}{a_i^{Na}} = \exp\left\{\frac{\mu_i^{o,\,Na} - \mu_i^{o,\gamma}}{RT}\right\} \qquad (3)$$

The second condition to be satisfied is the mass balance condition

$$M_i^{\gamma} + M_i^{Na} = M_i \text{ total} \qquad (4)$$

where M_i is the mass of the i th species.

The above equations must be solved for each species to fully characterize the volume element. However it is assumed for the sake of simplification that only carbon is transferring, therefore i = c where c denotes carbon.

The most restrictive assumption is perhaps that of graphite as the standard state. However, the form of the active carburizing species in the sodium is still a matter of debate,[2] and it is possible that several species contribute to carbon transfer. The attractive feature of defining the standard state as graphite is that the distribution coefficient a_i^{γ} / a_i^{Na} in Equation 3 can be set equal to unity.

3.0 COMPUTATIONAL PROCEDURE

Two sources of information have been used for basic thermodynamic data.[2,3]

1. The activity of carbon in an austenitic steel is given by Sawstrom and Hillert[2] as

$$RT\ln a_c^{\gamma} = RT\ln X_c^{\gamma} + ({}^{o}G_c^{\gamma} - {}^{o}G_c^{graphite}) + A_{Cr}^{\gamma} X_{Cr}^2 + B^{\gamma}(1-X_c)^2 + C_{Cr}^{\gamma} X_{Cr}(1-X_c) + C_{Ni}^{\gamma} X_{Ni}(1-X_c) \qquad (5)$$

Where: X_c^{γ} = mole fraction of C in γ (austenite)

X_{Ni} = mole fraction of nickel

X_{Cr} = mole fraction of chromium

T = absolute temperature in °K

The values for the constants in the equation are given as:[2]

$$({}^{\circ}G_c^{\gamma} - {}^{\circ}G_c^{graphite}) = 14381 + 3T$$

$$A_{Cr}^{\gamma} = 1300$$

$$B^{\gamma} = -3450 - 7.5T$$

$$C_{Cr}^{\gamma} = -27000$$

$$C_{Ni}^{\gamma} = 11000$$

2. The activity of carbon in sodium is given by Natesan and Kassner[3] as

$$RT \ln a_c^{Na} = RT \ln k\,(T)\, X_c^{Na} \qquad (6)$$

with k (T) chosen such that $a_c^{Na} = 1$ at saturation.

From Equation 6,

$$k\,(T) = \frac{1}{X_c^{Na\ Sat.}} \qquad (7)$$

For any temperature T, k (T) is given as,

$$[X_c^{Na\ Sat}(a/o)\ ]^{-1} = .0103 \quad \exp \frac{(13740)}{T} + .478 \qquad (8)$$

By equating Equations 5 with 6 we can obtain a term for X_c^{Na} at a particular temperature. In this case $T = T_{max}$ was selected.

$$X_c^{Na} = \frac{1}{k(T_{max})} \exp RT_{max} \ln X_c^{o} + (15206 + 3T_{max} + 1300X_{Cr}^{2}) - (3450 + 7.5T_{max})(1 - X_c^{o})^{2} - 27000X_{Cr}(1 - X_c^{o}) \qquad (9)$$

where: X_c^o is the equilibrium carbon content of the steel at $T = T_{max}$.

From Equation 6,

$$a_c^{Na} = k(T)X_c^{Na} \quad \text{with } X_c^{Na} = \text{const. by definition}$$

$\therefore$ X_c^{Na} <u>at any temperature T</u> is given by,

$$k\,(T)\ x\{\text{Equation 9}\} \tag{10}$$

We can now equate Equation 10 with 5 as

$$RT \ln a_c^{Na} = RT \ln a_c^{\gamma}$$

and substituting $\alpha(X_{Cr})$ for $27000\ X_{Cr} - 1300\ X_{Cr}^2 - 11756$

we obtain

$$\left(\frac{\gamma(X_{Cr})}{RT}\right)\left(1 - \frac{T}{T_{max}}\right) = \frac{\ln X_c^{\gamma}}{\ln X_c^o}\quad\left(\frac{T_{max}}{T}\right) \tag{11}$$

Solving for X_c^{γ} gives

$$X_c^{\gamma}\ (T) = X_c^o \frac{k(T)}{k(T_{max})}\ \exp\left(\frac{\alpha(X_{Cr})}{RT_{max}}\right)\ \exp\ \frac{\alpha(X_{Cr})}{RT} \tag{12}$$

All terms in Equation 12 are known except for X_c^o, the carbon content in the steel at T_{max}.

X_c^o is obtained from the mass balance (Equation 4).

Writing the mass balance for the entire system gives

$$\sum_{j=1}^{K} Mj\ + M^{Na} = M$$

where: j is the set of volume elements

M_c^{Na} = amount of carbon in the sodium

But $M_j = X_c^j \Delta V \cdot \zeta$ (ΔV = volume element)

ζ = factor for converting concentrations expressed as mole fraction to volume concentrations

$$\zeta \sum_{j=1}^{K} X_c^j \Delta V^j + M_c^{Na} = M_c \tag{13}$$

As M_c^{Na} is small relative to M_c^{γ} it can be ignored. Therefore, as $\Delta V \to 0$

$$\int_o^L X_c^{\gamma} \, dV = M$$

or $$\int_o^L \zeta \, X_c^{\circ}(T) \, A(x) \, d\gamma = M = \bar{X}_c V \zeta \tag{14}$$

where $\bar{X}$ the initial average concentration and V = total volume of steel used in the system.

Substituting Equation 12 into 14 and solving for X_c° gives

$$X_c^{\circ} = \bar{X}V \Big/ \int_{x=o}^{L} \frac{k(T)}{k(T_{max})} \exp\left\{\frac{-\alpha(X_{Cr})}{RT_{max}}\right\} \exp \frac{\alpha(X_{Cr})}{RT(x)} \, A(x)dx$$

Thus the solution to Equation 15 gives X_c° the carbon content at T_{max}.

Use of Equation 12 then gives X_c^{γ} for any temperature, and Equation 9 gives X_c^{Na} .

4.0 REFERENCES

1. K. G. Denbigh, The Principles of Chemical Equilibrium, Cambridge University Press, New York, 1961.

2. C. Stawstrom and M. Hillert, "Improved Depleted-Zone Theory of Intergranular Corrosion of 18-8 Stainless Steel," J. Iron Steel Inst. London 207, Pt. 1, pp. 77-85 (1969).

3. K. Natesan and T. F. Kassner, "Calculations of the Thermodynamic Driving Force for Carbon Transport in Sodium-Steel Systems," ANL-7646, December 1969.

APPENDIX B

DETERMINATION OF CARBON GRADIENTS IN STAINLESS STEEL AFTER EXPOSURE TO A LIQUID METAL ENVIRONMENT

C. Bagnall

1.0 INTRODUCTION

During the past year, a continuing search and up-dating of the literature on carbon diffusion in stainless steel alloys has been conducted. This appendix discusses theoretical and experimental determinations of carbon gradients and carbon diffusivities in stainless steel after prolonged elevated temperature exposure to a liquid metal environment. The results and methods outlined in this appendix are essentially those used to estimate carbon transfer rates and depths of depletion in FFTF components. The importance and effect of various assumptions on the results and some general points contributing to error are briefly discussed. A simplified method of carbon gradient calculation is also presented.

2.0 THEORETICAL CARBON GRADIENTS

The following equation (derived from Ficks law) may be used to describe the concentration of carbon $C_{(x,t)}$ at any point, x, within the wall of a tube after a given time, t:

$$C_{(x,t)} = C_e + 4\frac{(C_o - C_e)}{\pi}\left[\sum_{n=1}^{\infty}\frac{(-1)^{n-1}}{(2n-1)}\exp\left[-(2n-1)\frac{2\pi^2 Dt}{a^2}\right]\frac{\cos(2n-1)\pi x}{a}\right] \quad (1)$$

where: C_o = Initial carbon concentration

C_e = Equilibrium surface concentration

D = Diffusion Coefficient

The equation pertains to a system in which the rate of carbon movement is controlled entirely by the diffusion resistance; interfacial or internal kinetic resistances are considered negligible. Also, it is assumed that the diffusion coefficient, D, is not dependent on the concentration of the diffusing species, i.e., $D \neq f(D_{x,t})$. To estimate depletion depths and the shape of the carbon concentration gradient, a computer program was set up to solve the equation (summing the first ten terms in the series) for carbon concentration at ten equal intervals throughout a tube wall, using the following parameters:

Constant temperature, T	= 1050°F
Period of exposure, t,	= 2.195×10^5 (25 years)
Initial Carbon Concentration, C_o	= 600 ppm
Equilibrium Surface Concentration, C_e	= 100 ppm (arbitrary value)[a]
Tube wall thickness, a/2	= 0.125", 0.500", 0.750", 1.000"
Diffusion Coefficient, D,	= 0.25×10^{-7} cm^2hr^{-1}, 0.25×10^{-6} cm^2hr^{-1}, 0.25×10^{-5} cm^2hr^{-1}

The wall thicknesses used in this calculation represent the range of wall thicknesses encountered in many of the FFTF structural components. Also, as discussed later, the values used for the diffusion coefficient approximately represent the scatter band reported in the literature for carbon movement in stainless steels.

A profile of carbon concentration across a tube wall is plotted graphically in Figures B-1 and B-2 for the various combinations of these data.

3.0 DETERMINATION OF D, THE DIFFUSION COEFFICIENT OF CARBON

There are varying reports regarding the value of diffusivity of carbon in austenitic stainless steel. In spite of the fact that D is a physical property of the material, values obtained vary over several orders of magnitude. This section reviews the data and results of three experimenters, whose work was directed at interstitial diffusivity determinations in Types 316 and 304 stainless steel when exposed to a liquid metal environment.[1,2,3]

3.1 Data Documented By Walker et al. (1966)[1] (See Figure B-3, Point A)

Nitrogen gradients were measured in stainless steel specimens inserted in a liquid potassium loop over temperatures ranging from 1200-1500°F. Diffusion coefficients were calculated from these data and a linear plot of lnD against the reciprocal of the absolute temperature constructed. The diffusion coefficient of carbon was calculated at 1500°F using data obtained from analysis of successive layers of the decarburized tube wall. This point was then used to construct a diffusion curve for carbon parallel to that derived for nitrogen, assuming that diffusion rates of the two similar atoms would exhibit approximately the same temperature dependency.

[a] The effect of the value of C_e on D is discussed in Section 4.0.

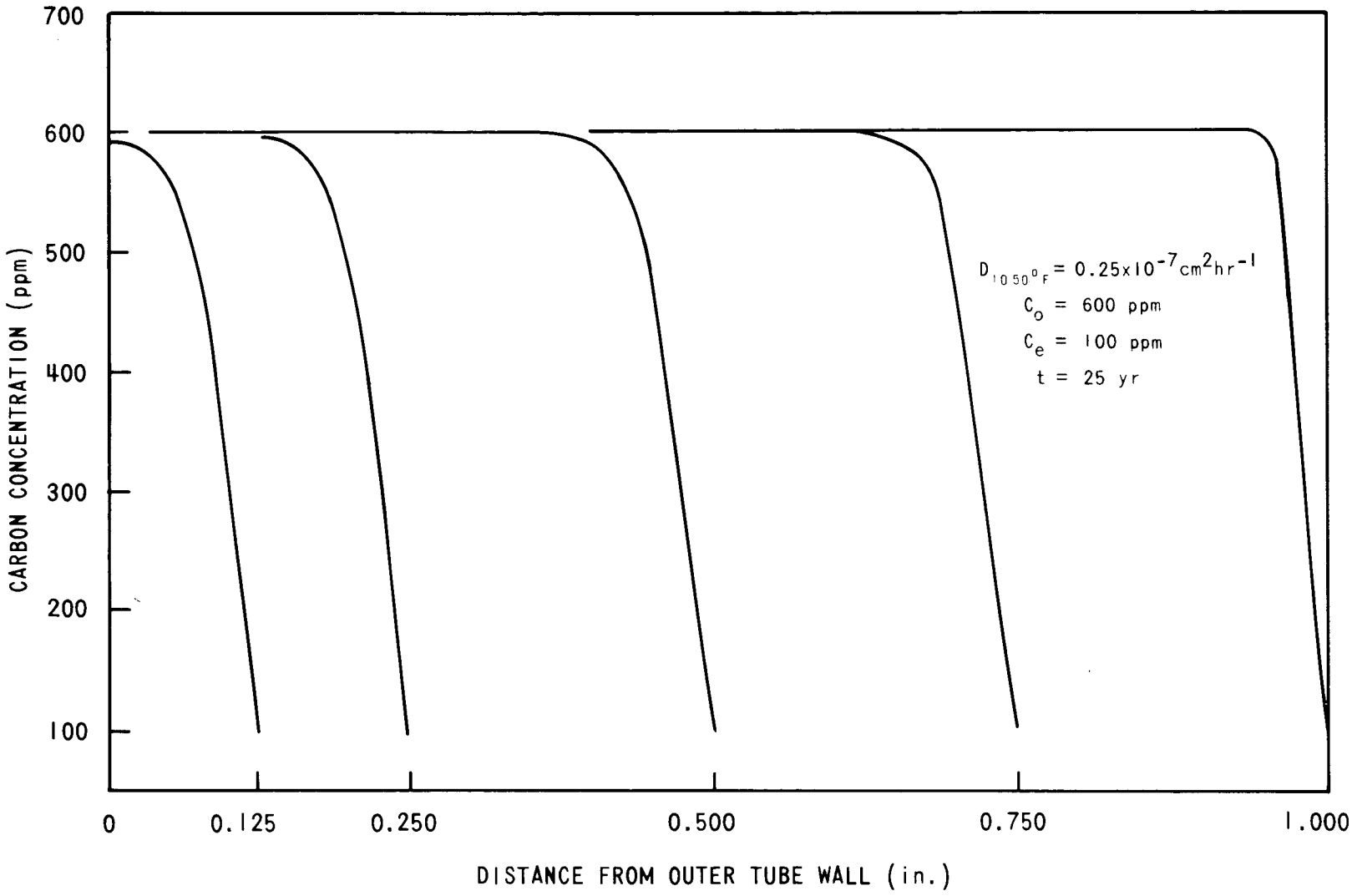

Figure B-1. Carbon Concentration Curves for Various Tube Wall Thicknesses for Type 316 Stainless Steel Exposed at 1050°F

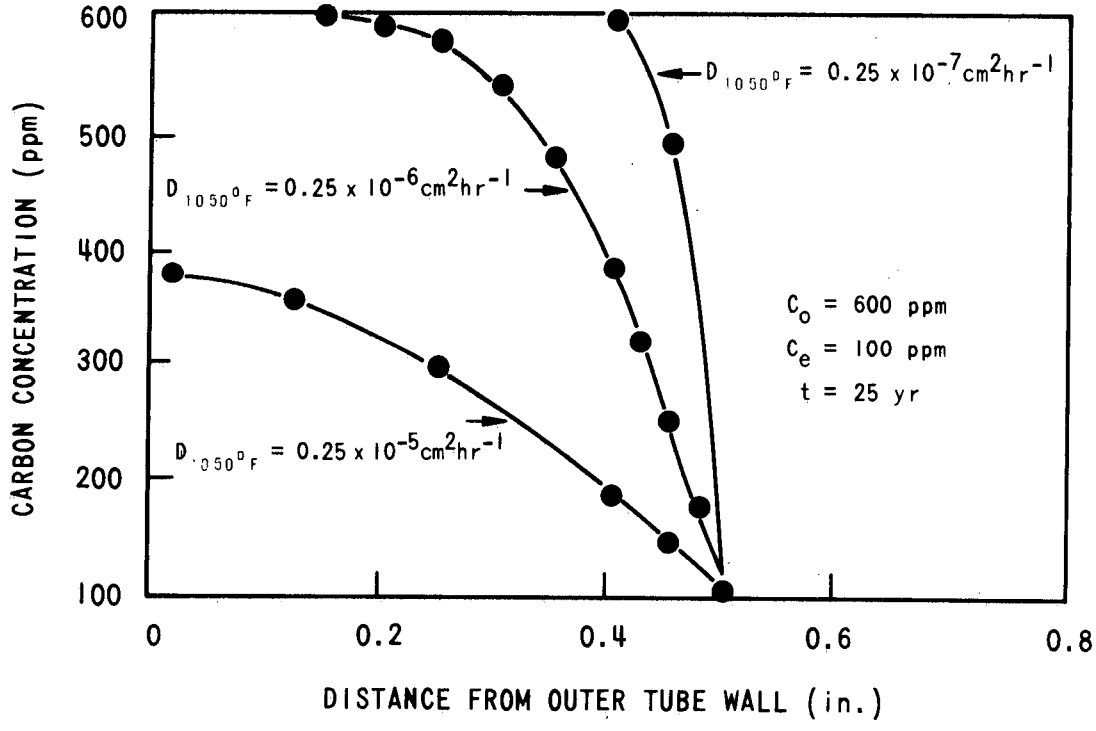

Figure B-2. Carbon Concentration Curves Through a 1/2 Inch Tube Wall, for Various Values of Carbon Diffusion at 1050°F (Type 316 Stainless Steel)

3992-5

The linear plot of lnD vs. 1/T for nitrogen was constructed from four experimental gradient analyses between 1200°F and 1500°F using Equation 1 with appropriate boundary conditions. The plot for carbon shown in Figure B-3, therefore, depends on these four data points and the single carbon analysis at 1500°F for its accuracy. Provided the value for the diffusity of carbon at 1500°F is reliable, extrapolation over the 1200-1500°F temperature range should introduce minimal error, on the reasonable assumption that the similarity of carbon and nitrogen atoms will lead to similar rates of diffusion. Extrapolation below 1200°F, however, should be treated with some caution, since the original data are so limited.

3.2 Data Documented By Plumlee et al. (1965)[2] (See Figure B-3, Point B)

Two small rods, 3/4-inch diameter and 3-1/2-inch long, machined from Type 316 stainless steel were placed in an isothermal test loop so that one rod was upstream of a carbon source and the other downstream. After a test run, the samples were incrementally machined and analyzed for carbon (1/2g samples). Diffusion calculations were made from data obtained at temperatures between 838°F and 1051°F under the basic assumption that carbon concentrations in the sodium remained constant throughout any test.

The following points were noted:

1. Oxygen levels in the sodium for the tests varied from 10 to 77 ppm.

2. Carbon concentration in the carbon sources (carburized AISI-1012 carbon steel sheet, 18-mil thick wound into a spiral) varied from 1.1 to 1.6 w/o.

3. With a flow rate of one gpm, there was a marked difference between carbon pick-up in upstream and downstream specimens, the former always being less than the latter. In preliminary tests at eight gpm, no positional effects were observed.

The reliability of data obtained in these experiments is somewhat uncertain, because of non-uniform loop operating conditions and the cylindrical geometry of the specimens. Machining consecutive layers from the rods to give half-gram samples required an increasing depth of cut for each layer so that mean carbon concentration calculations were made for different radial thicknesses.

The values obtained for extrapolated surface carbon contents (C_e values) were dependent upon specimen location. The variation in calculated values of D between upstream and downstream specimens is given in Table B-1. Average values determined from each pair of figures at each temperature were used to plot the lnD vs. 1/T curve given in the paper.

It is reasonable to assume that the specimens placed downstream from the carbon source would reach in time an equilibrium condition with the carbon-

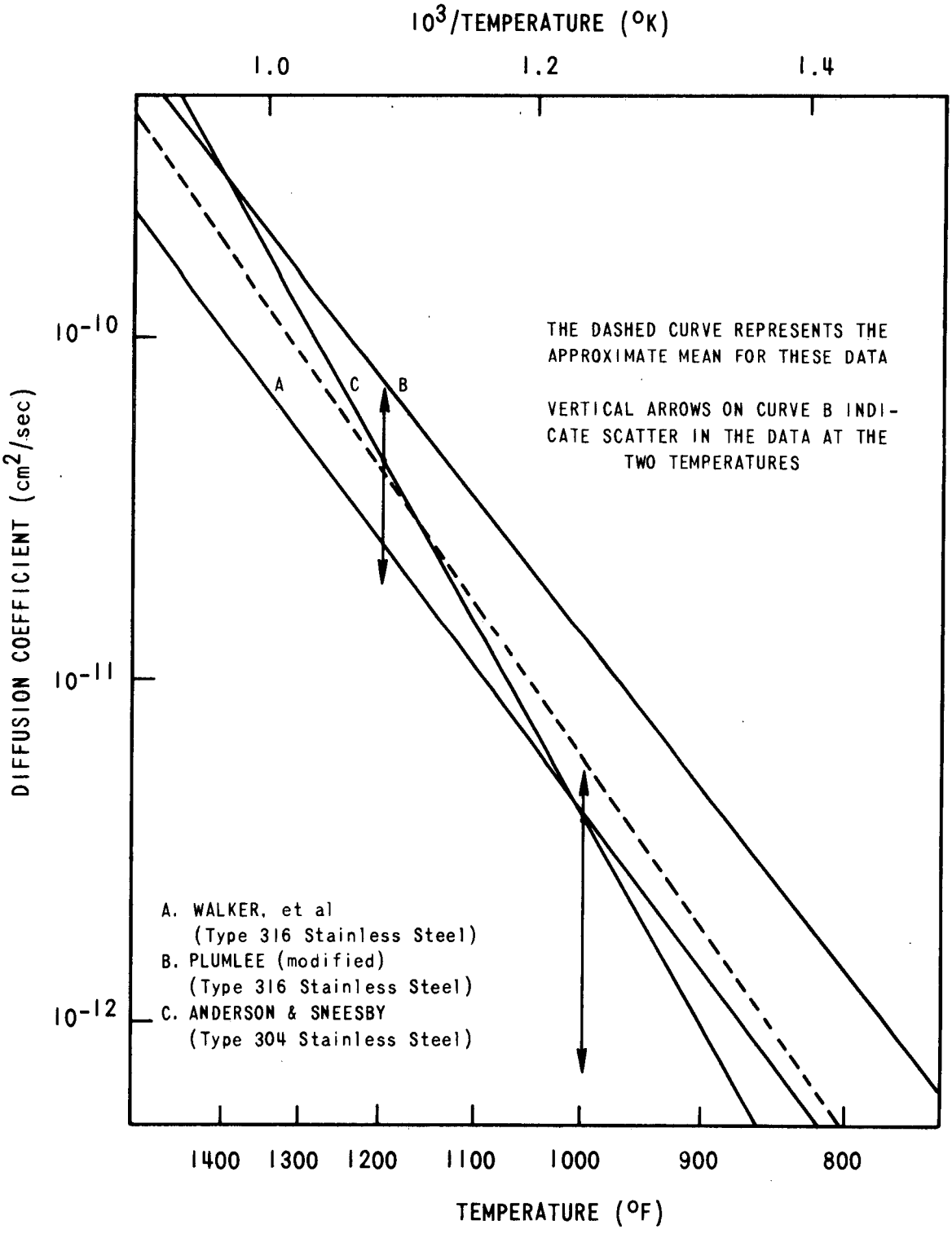

Figure B-3. Diffusivity of Carbon in Austenitic Stainless Steels From Experiments Conducted in a Liquid Metal Environment

3992-6

Table B-1. Calculated Diffusion Coefficients Of Carbon In 316 Stainless Steel (After Plumlee)		
Temp. (°F)	Sample position with Respect to Carbon Source	Diff. Coef., D ($cm^2/sec.$)
838	Upstream	1.5×10^{-12}
	Downstream	2.4×10^{-12}
843	Upstream	1.3×10^{-12}
	Downstream	1.9×10^{-12}
940	Downstream	11×10^{-12}
944	Upstream	6.7×10^{-12}
	Downstream	7.2×10^{-12}
1051	Downstream	18×10^{-12}
Base Carbon Content of Samples 0.05 w/o		

saturated sodium. The specimens placed upstream of the source will reach an equilibrium condition also, but after passage of the sodium round the loop, this equilibrium may be different from the downstream equilibrium condition. In Figure B-3, data from the downstream specimens have been plotted on their own with the result that diffusion rate increases less rapidly with increasing temperature than indicated in the paper.

This new curve is almost parallel to that given by Walker.

3.3 Data Documented by Anderson and Snessby (1960)[3] (See Figure B-3 Point C)

Although the work of these authors concentrates upon carburization of Type 304 stainless steel, the material is so close in composition to Type 316 stainless steel that it is unlikely that diffusivity values will change by as much as an order of magnitude from one to the other. Figure B-4 shows the composition fields of each alloy plotted on a Schaeffler diagram; Type 304 stainless steel may contain up to 10% ferrite, which in general will be twice the amount found in Type 316 stainless steel. But the phase will be present predominantly at grain boundaries where diffusion rates are in any event one or two orders of magnitude higher than in the matrix. So unless there is sufficient ferrite present and a sufficiently large grain size to permit the continuous formation of ferritic networks,

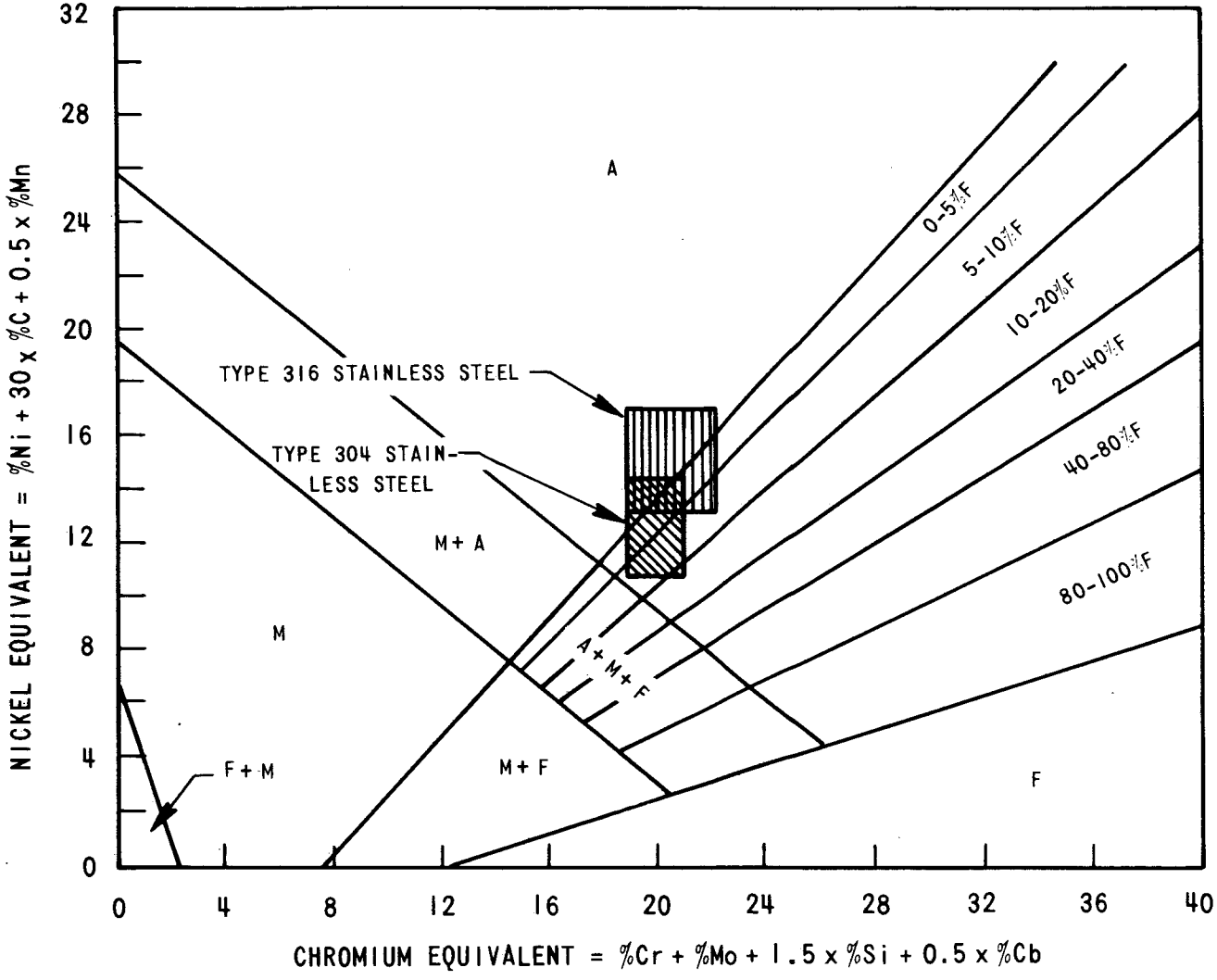

Figure B-4. Composition Fields of Type 304 and Type 316 Stainless Steel; Schaeffler Diagram

the overall effect of the phase will be minimal. The presence of molybdenum in Type 316 stainless steel as a carbide stabilizing element is also not likely to significantly affect the overall movement of carbon through the austenitic matrix.

Most of the specimens were not exposed in a loop system but were encapsulated with sodium in Type 304 stainless steel tubing, 1-1/2-inch OD with a 0.065-inch wall and 3 to 6-inch length. The capsules were inclined at an angle of 30° and rotated in the furnace at 15 rpm. However, some specimens were suspended in "small sodium test loops being operated for other experiments;" distinction between these two exposure methods is not indicated in the reported data.

Three major factors affecting diffusion rates were considered for this work.

Concentration Gradients

The difference between the carbon concentration of the surface in equilibrium with carbon saturated sodium and the initial carbon content of the steel was considered a major controlling factor in the rate of carbon diffusion. For long exposure times, the assumption was made that the specimen surface in contact with the sodium would come to instantaneous equilibrium. For these experiments, the assumption was found to be satisfactory for exposure times of one hour or greater.

Specimen Geometry

The size and shape of a specimen contributes significantly to carburization rates. Thin sheet specimens were chosen for this work so that edge, corner, and other peripheral effects prominent in specimens of more solid geometry, could be ignored. Care was taken to ensure that for any calculation of D, the specimen thickness was at least twice the total depth of the carburized zone. A concentration gradient in a specimen thinner than this minimum would be modified.

Temperature

Temperature control was considered important for establishing surface concentration of the diffusing element when in equilibrium with the source.

In microstructural studies, the authors observed that carburization proceeded to a greater depth at grain boundaries, but found that this separate diffusion rate accounted for a negligible portion of overall carbon gain. They observed, metallographically, that increasing temperature caused a decrease in the structural effect on diffusion. Carburization rates were determined in the following ways:

Chemical Analysis

Several sheet specimens varying in thickness from 0.002 to 0.030 inch were exposed to carbon-saturated sodium for a given (relatively short) period of time at a temperature of 1200°F and then analyzed to determine the average carbon concentration of each specimen. The plot of average carbon concentration vs. thickness was extrapolated to zero thickness to determine the surface (equilibrium) concentration. An approximate value of D at 1200°F was then calculated from the expression:

$$D = \left(\frac{C_m - C_o}{C_s - C_o} \times \frac{L}{K\sqrt{t}} \right)^2 \qquad (2)$$

Where: C_m = average carbon concentration after exposure

C_s = surface carbon concentration after exposure

C_o = initial carbon concentration

K = geometrical constant, equal to $2/\sqrt{\pi}$

L = 1/2 the specimen thickness

t = time of exposure

The equation was applied only to specimens which were thicker than twice the diffusion depth.

The value of C_s was further refined by using this approximate value of D in the expression:

$$L = \left[\frac{Dt}{A - B \log 1 - \frac{C_n - C_o}{C_s - C_o}} \right]^{1/2} \qquad (3)$$

A and B are constants equal to 0.0851 and 0.993 resp.

to determine for what thickness specimens would have an overall carbon gain equal to 99% of the (extrapolated) surface carbon gain. The average carbon concentration for all specimens at and below this minimum thickness was calculated, and after adjustment to the 100% equilvalent, this was taken as the true value for carbon surface concentration. A new value of D was then determined.

Justification for this latter manipulation is presumably founded upon the initial graphical extrapolation for C_s, which was highly imaginative and certainly did not represent a smooth extension of the experimentally determined part of the concentration curve.

Metallographic Examination

The relationship derived by Darken and Gurry between the concentration function $(C-C_o)/(C_o-C_o)$ and the dimensionless variable $x/(Dt)^{1/2}$ (this is discussed in Section 4.0) was used in graphical form to determine carbon concentrations C, at metallographically detectable case depths, x, using the previously determined values of D, C_s, and C_o.

With values of concentration so calculated, a series of curves were constructed relating case depth with time at various temperatures.

Hardness Measurements

A parallel type of calculation on hardness data indicated that 300 khn corresponded to a carbon content of 0.19%. This value was taken as the limit of the carburized case for all specimens. Case depths determined from both hardness and metallurgical measurement were then used to calculate diffusion coefficients at various temperatures.

Results from these three methods of calculating diffusion coefficients graph of lnD vs. 1/T, as shown in Figure B-3.

The following points were noted:

1. The straight line shown in Figure B-5 appears to have been drawn using "average" chemical analyses at 1200 and 1000°F only. The range of D values obtained at these temperatures varied from 0.2 to 0.7 x 10^{-10} cm^2sec^{-1} for the former and from 0.7 x 10^{-12} to 0.6 x 10^{-11} cm^2sec^{-1} for the latter. This straight line was then extended through the temperature range for which case depths were measured.

2. A good correlation between hardness data at 1200°F and carbon content was established, suggesting that at this temperature hardness measurements could be used to check chemical analysis results (and also as an indirect method of determining carbon concentration of a sodium system). However, the usefulness of this relationship would appear to be confined to a carburizing system and to the lower temperature ranges, since above 1250°F as the authors indicate, correlation between carbon content and hardness becomes too dependent on time of exposure to be reliable.

3. Diffusion rates were found to be lower at lower temperature than those reported for Type 316 stainless steel material.

The data obtained by Anderson and Sneesby for the coefficient of diffusion of carbon in Type 304 stainless steel at 1200°F as determined by chemical analysis of carburized specimens, supports data similarly obtained by other workers. However, the slope of the D vs. 1/T curve

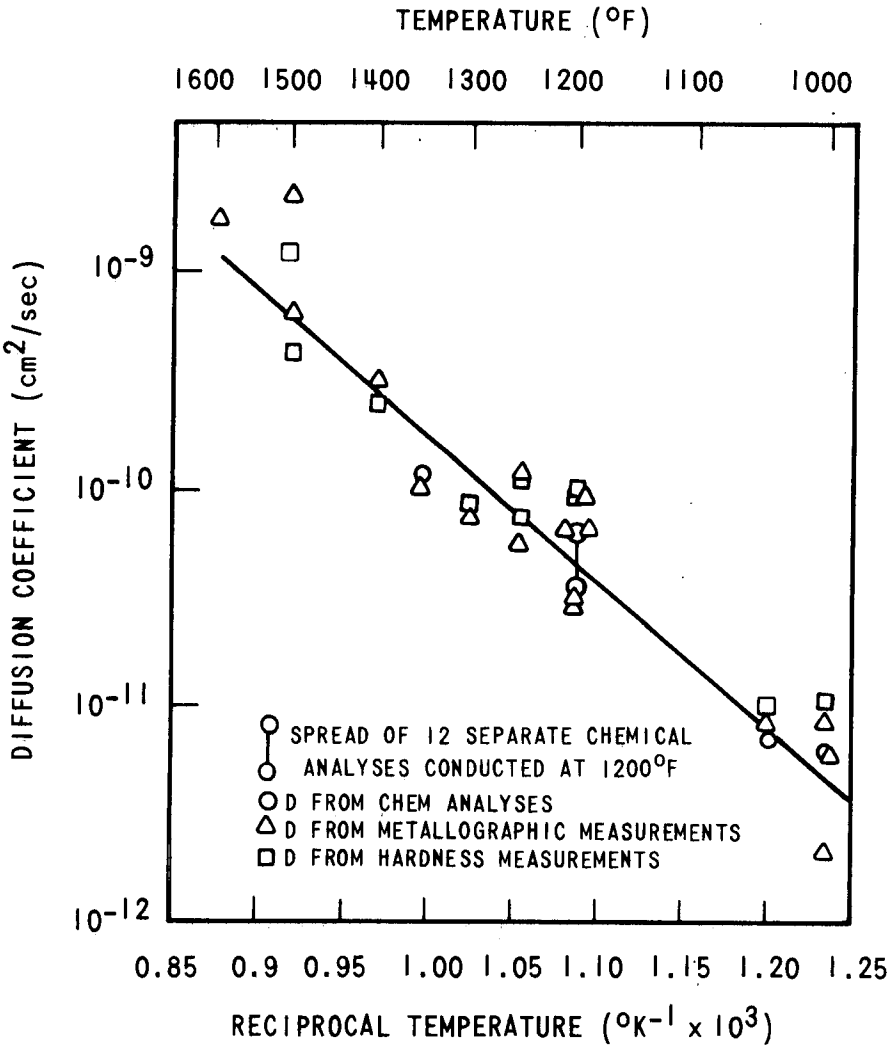

Figure B-5. Diffusion Coefficient of Carbon Versus 1/Absolute Temperature for Type 304 Stainless Steel (After Anderson and Sneesby)

3992-8

cannot be considered too precise, since it was largely established by metallographic and hardness measurements. Although there is no discussion of possible degree of error contributed by the various forms of measurement, some idea of its magnitude may be gained by observing the scatter of 1200°F (Figure B-5).

3.4 Summary

The three experiments described above for the study of carbon diffusion are the only ones currently reported in the literature in which data were obtained by exposing specimens to a liquid metal environment. One of the experiments deals with specimen decarburization and the other two with carburization, and each includes a source of error which may arise either from an assumption or from experimental procedure. Yet, the diffusion data calculated from the three (after modifying Plumlee's data) are within a factor of three of one another above 1000°F.

The mean curve for the above data is shown in Figure B-6, together with carbon diffusion data for other austenitic materials determined out of a liquid metal environment.[4,5,6,7] Two striking features are apparent: the temperature dependence of the diffusion coefficient is much less in the liquid metal environment experiments, and its value is lower at temperatures above 1000°F. At 1300°F, the out-of-sodium data are spread over two orders of magnitude above this mean curve.

One further piece of experimental evidence to support this mean curve for carbon diffusion is derived from some work at ANL.[8] In this work, Type 304 stainless steel rods were exposed to "impure" sodium at 1200°F for one week. The results indicate that the diffusivity of carbon at this temperature is 0.61×10^{-10} $cm^2 sec^{-1}$;(a) as shown in Figure B-6, this value falls near the mean curve derived from the work in liquid metal described above.

The discrepancy between the two sets of diffusion data (in and out-of a liquid metal environment) is difficult to justify or explain on theoretical grounds. The diffusion coefficient of an element in a given material is a constant of that material and should not be dependent upon method of measurement or external environment. However, stainless steel microstructure in the temperature range 1000 - 1400°F is in a constant state of change, and many of its physical properties experience a radical alteration so that the material itself may be considered as a variable. Why this is not reflected as a break in the Arrhenius plot of diffusivity vs. temperature is not clear; the plot should not be linear at all if the material really does alter significantly. Why a sodium environment should apparently slow down carbon movement in the material is also confusing. At present, it is only possible to conclude that it is not a diffusion coefficient that is measured at all, but rather an overall reaction rate for carbon in a given alloy in a given environment.

(a) Calculation of this value is given in Section 4.0.

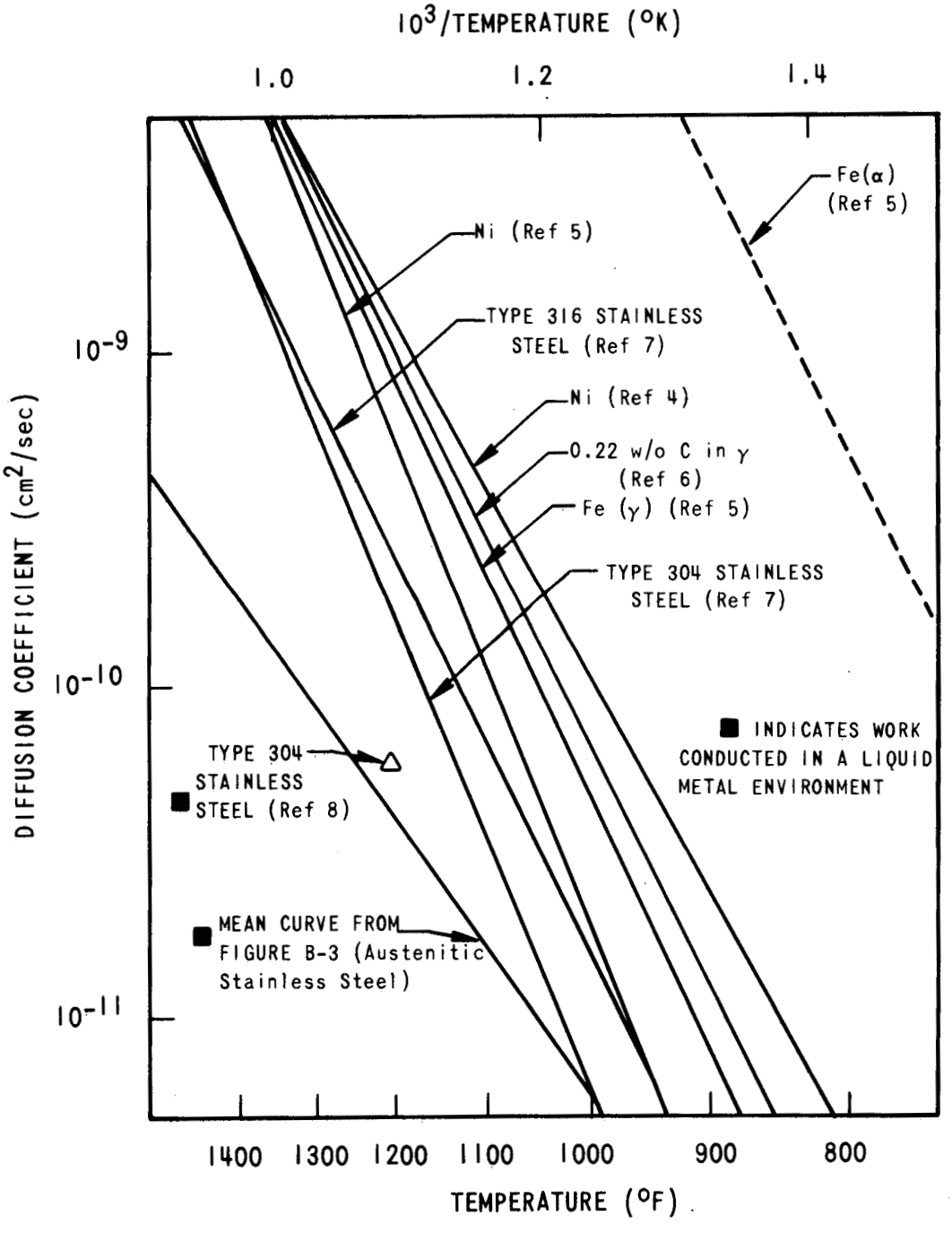

Figure B-6. Diffusivity of Carbon in Austenitic Matrices; a Comparison of Available Data, and of Work Conducted in and out of a Liquid Metal Environment

3992-9

4.0 A SIMPLIFIED METHOD FOR CARBON GRADIENT CALCULATION

The problem of determining the distribution of a diffusing element after any given time is discussed in some detail by Darken and Gurry.[9] Mathematically, this involves the integration of the partial differential equation describing Ficks second law:

$$\frac{\partial C}{\partial t} = D \frac{\partial^2 C}{\partial x} \qquad (4)$$

so that the boundary conditions of initial uniform composition, C_o, and instantaneous initial surface equilibrium concentration, C_s, are satisfied; i.e.,

$C = C_o$ at $t = 0$, and $0 > x > \infty$

$C = C_s$ at $x = 0$, and $0 > t > \infty$

Equation 4 has a solution to its integration in the form of an error function, ϕ, which may be written

$$1 - \phi = \text{erf} \frac{x}{2\sqrt{Dt}} = \frac{C - C_o}{C_s - C_o} \qquad (5)$$

From this expression, the concentration fraction is a function only of the single dimensionless variable, $x/\sqrt{Dt}$. Hence, a plot of concentration against distance is precisely the same form at all times; i.e., any one curve may be imagined as obtained from any other by stretching or contracting the abscissa.

From a plot of $(C-C_o)/(C_s-C_o)$ vs. $x/\sqrt{Dt}$, it is found that when $(C-C_o)/(C_s-C_o) = 0.5000$, $x/\sqrt{Dt} = 0.9538$. Thus, we may make the approximation that when concentration of the diffusing element is midway between initial and ultimate values (i.e., at $1/2\ (C_o+C_s)$, the distance x of this plane from the surface, at which concentration is C_s, is equal to $\sqrt{Dt}$. Using this information, we may construct approximate diffusion curves for those shown in Figure B-2 using Table B-2.

Two points are plotted for each value of D: one for the tube surface where concentration = C_s, and the other for $1/2\ (C_s+C_o)$ where $x = \sqrt{Dt}$, as given in Table B-2. A straight line is constructed through these two points to the intersection of the horizontal line of original concentration, C_o. The three curves are shown in Figure B-7, together with the computed curves of Figure B-2.

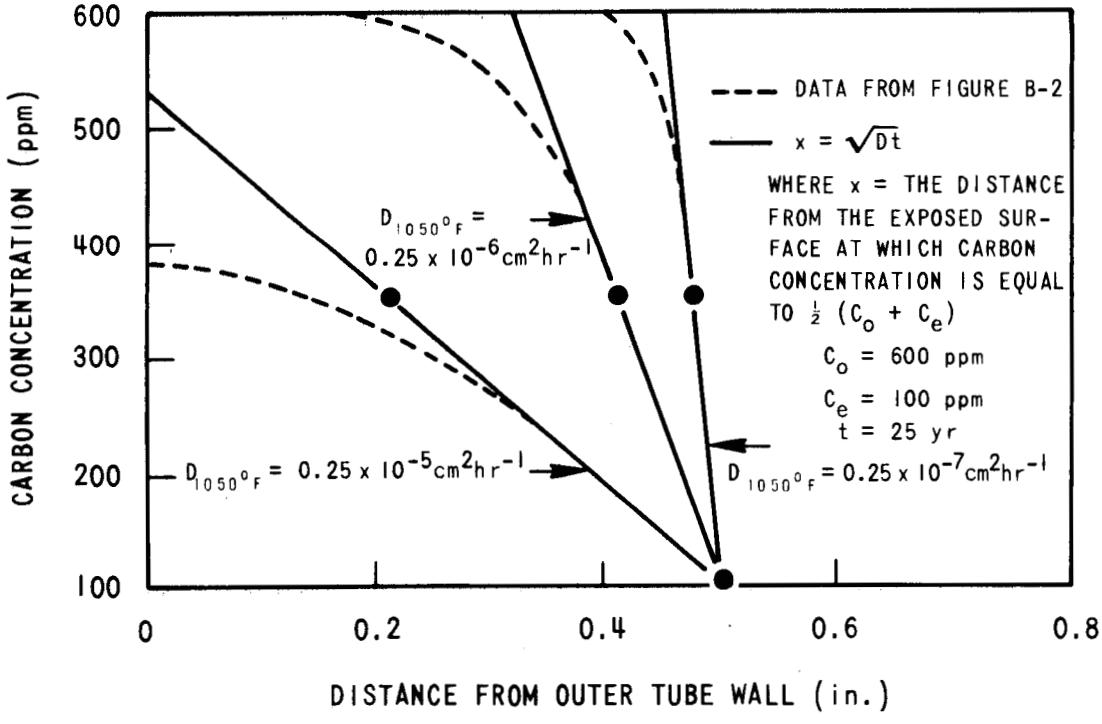

Figure B-7. Comparison of Computed Concentration Curves and Approximated Curves for Three Values of Carbon Diffusion in Type 316 Stainless Steel at 1050°F

3992-10

Table B-2. Values For x When $(C-C_o)/C_s-C_o)$ = 1/2, For Various Values Of D				
D (cm^2 hr^{-1})	t (hr)	Dt_2 (cm^2)	$x=\sqrt{Dt}$ (cm)	x (in.)
$0.25.10^{-7}$	$2.195.10^{-5}$	$0.548.10^{-2}$	0.074	0.029
$0.25.10^{-6}$	$2.195.10^{5}$	$0.548.10^{-1}$	0.234	0.092
$0.25.10^{-5}$	$2.195.10^{5}$	0.548	0.740	0.291

The major divergence between the computed and approximated curves occurs as the value of C_o is approached. Carbon depletion at this level will not seriously effect material properties and will be comparable to normal concentration fluctuations within the bulk of the material.

The good overall agreement between the two sets of curves suggest that the approximate method of calculation could be used for determinations of element gradients at the surface of a material, given the exposure conditions and appropriate diffusion coefficients.

As a further example of application of the method the work referenced in Section 3.0[8] may be used to obtain an approximate value for D at 1200°F as follows.

A type 304 stainless steel rod was exposed in sodium for a period of one week. The report mentions that "surface layers, to a depth of about 4×10^{-3} inch, had carbon concentrations of about 0.070 w/o. Specimen layers from 6-12 mils in depth showed gradually reduced carbon content, from 0.056 to 0.052 w/o." Figure B-8 shows a plot of these data; concentrations at the mean of the first four mils, and at six and twelve mil depths are plotted as given, and these three points are used to extrapolate the curve to obtain a surface carbon concentration.

Using the relation:

$$D = \frac{x^2}{t}, \text{ where } x = \text{depth at which concentration equals } 1/2(C_o+C_s)$$

From Figure B-8, taking C_o = 520 ppm, C_s = 830 ppm, then x = 2.4 mils at 1/2 (C_o+C_s) (= 675 ppm).

$$\text{hence, } D = \frac{(2.4 \times 2.54 \times 10^{-3})}{7 \times 24 \times 3600} \text{ cm}^2 \text{ sec}^{-1}$$

$$= 0.61 \times 10^{-10} \text{ cm}^2 \text{ sec}^{-1}$$

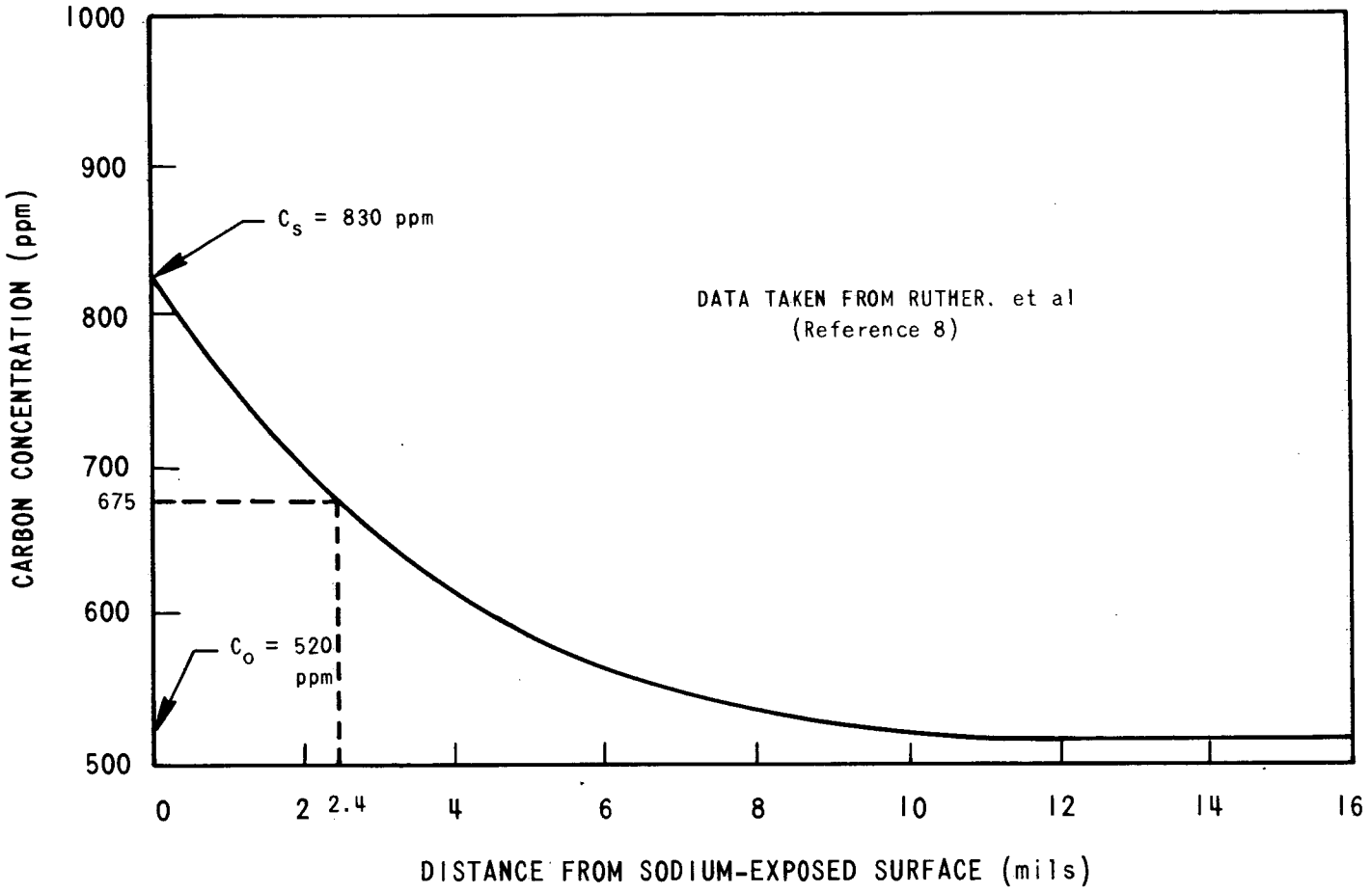

Figure B-8. Plot of Carbon Concentration Versus Distance From the Surface of a Type 304 Stainless Steel Rod Exposed to Sodium at 1200°F

This value is plotted on Figure B-6 and shows good agreement with the mean curve derived from other work conducted in a liquid metal environment. The importance of this illustration is to show that even with a minimum of data, useful information can be gained concerning rate of carbon movement; the figures may be approximate but should not be in error by as much as an order of magnitude.

One further point should be mentioned regarding the measurement of surface (equilibrium) concentrations and the depth of the zone experiencing change due to diffusion into or out of a material. Suppose after time t at constant temperature T, a given material loses a quantity of some element by a diffusion process across a boundary. The situation may be represented graphically as shown in Figure B-9. A composition gradient is established over some distance X from the boundary concentration of the element, C_s, to the initial concentration, C_o, in the bulk material.

At temperature T, the diffusivity D of the element may be determined from manipulation of the error function,

$$C_{(x,t)} = C_o \text{ erf } \frac{x}{2\sqrt{Dt}}$$

using the relation as before that

$$D = \frac{x^2}{t}, \text{ when } x = \frac{X}{2}$$

X is dependent only on t, and not on C_s.

At any given temperature, therefore, depth of depletion will increase with time, but will not be affected by the surface concentration.

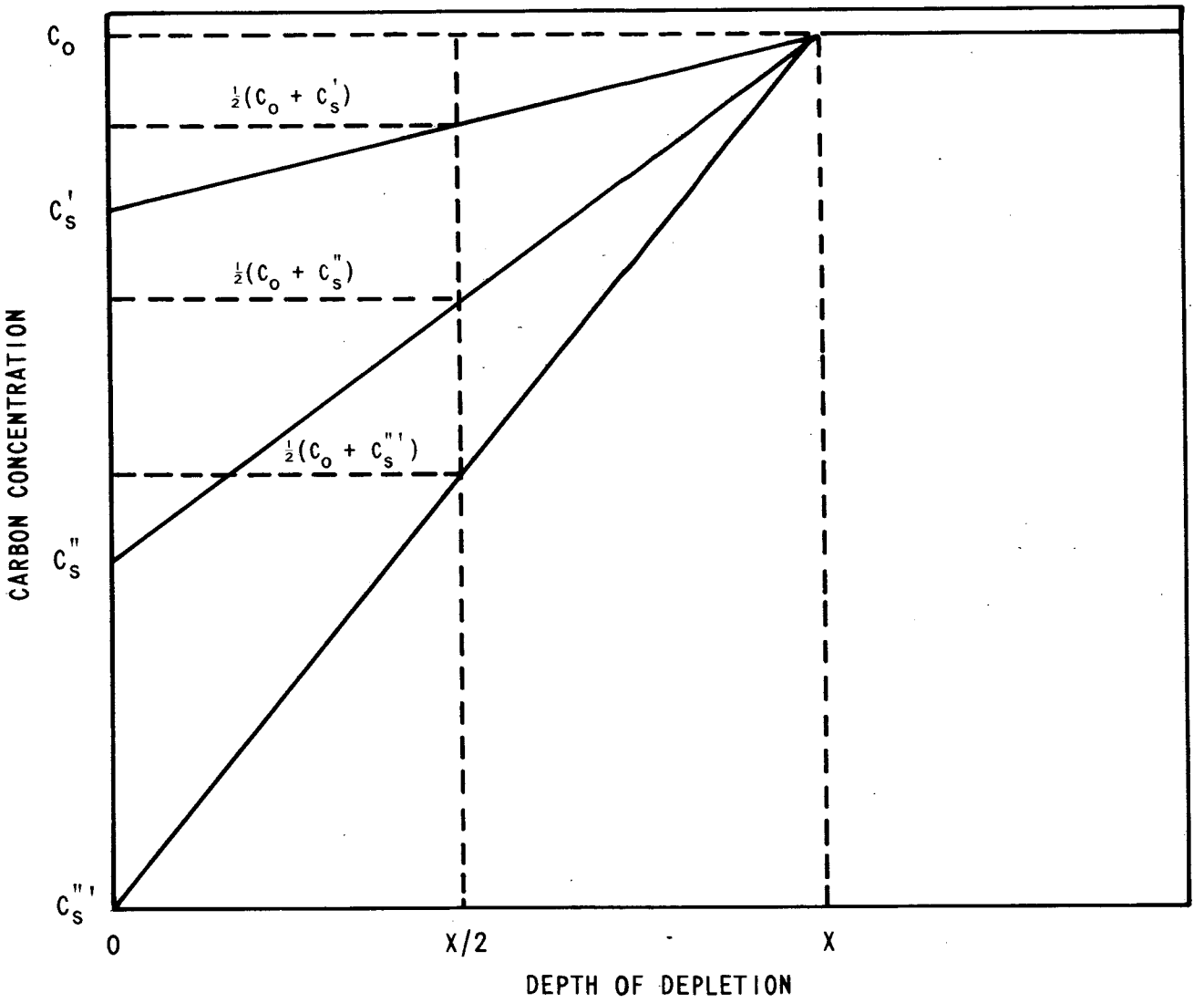

Figure B-9. Theoretical Composition Gradients Established at Constant Temperature After a Given Time, for a Diffusing Element for Various Boundary Concentrations, C_S

5.0 REFERENCES

1. "Investigation of Bimetallic Liquid Metal Systems, Final Report," GMAD-3643-8, September 1966.

2. D. E. Plumlee, R. W. Lockhart, L. E. Pohl, and T. A. Lauritzen, "Sodium Mass Transfer. XVIII. Extended Studies of Carbon Movement in Pumped Sodium Test Loops," GEAP-4834, June 1965.

3. W. J. Anderson and G. V. Sneesby, "Carburization of Austenitic Stainless Steel in Liquid Sodium," NAA-SR-5282, September 1960.

4. R. P. Smith, "The Diffusivity of Carbon in Gamma Iron-Nickel Alloys," Trans. Met. Soc. AIME 236, pp. 1224-1227 (1966).

5. "Carbon Meter for Sodium. Progress Report, February 21-June 30, 1966," UNC-5160, July 1966.

6. C. Wells, W. Batz, and R. F. Mehl, "Diffusion Coefficient of Carbon in Austenite," J. Metals 188, pp. 553-560 (1950).

7. R. P. Agarwala, M. C. Naik, M. S. Anand, and A. R. Paul, "Diffusion of Carbon in Stainless Steels," J. Nucl. Mater. 36, pp. 41-47 (1970).

8. W. E. Ruther and others, "Interactions of Type 304 Stainless Steel with Impure Sodium," in "Annual Progress Report for 1967. Metallurgy Division," ANL-7417, pp. 11-12.

9. L. S. Darken and R. W. Gurry, Physical Chemistry of Metals, McGraw-Hill, New York, 1953.